

## Video Article

# Simultaneous Multi-surface Anodizations and Stair-like Reverse Biases Detachment of Anodic Aluminum Oxides in Sulfuric and Oxalic Acid Electrolyte

Healin Im<sup>\*1</sup>, Seok Hwan Jeong<sup>\*1</sup>, Dong Hyuk Park<sup>2</sup>, Sunkook Kim<sup>1</sup>, Young Ki Hong<sup>1</sup><sup>1</sup>School of Advanced Materials Science and Engineering, Sungkyunkwan University<sup>2</sup>Department of Applied Organic Materials Engineering, Inha University<sup>\*</sup>These authors contributed equallyCorrespondence to: Dong Hyuk Park at [donghyuk@inha.ac.kr](mailto:donghyuk@inha.ac.kr), Young Ki Hong at [imhyke0419@gmail.com](mailto:imhyke0419@gmail.com)URL: <https://www.jove.com/video/56432>DOI: [doi:10.3791/56432](https://doi.org/10.3791/56432)

Keywords: Engineering, Issue 128, Simultaneous multi-surfaces anodizations, stair-like reverse biases, direct detachment, anodic aluminum oxide, mass-production, green technology

Date Published: 10/5/2017

Citation: Im, H., Jeong, S.H., Park, D.H., Kim, S., Hong, Y.K. Simultaneous Multi-surface Anodizations and Stair-like Reverse Biases Detachment of Anodic Aluminum Oxides in Sulfuric and Oxalic Acid Electrolyte. *J. Vis. Exp.* (128), e56432, doi:10.3791/56432 (2017).

## Abstract

After reporting on the two-step anodization, nanoporous anodic aluminum oxides (AAOs) have been widely utilized in the versatile fields of fundamental sciences and industrial applications owing to their periodic arrangement of nanopores with relatively high aspect ratio. However, the techniques reported so far, which could be only valid for mono-surface anodization, show critical disadvantages, *i.e.*, time-consuming as well as complicated procedures, requiring toxic chemicals, and wasting valuable natural resources. In this paper, we demonstrate a facile, efficient, and environmentally clean method to fabricate nanoporous AAOs in sulfuric and oxalic acid electrolytes, which can overcome the limitations that result from conventional AAO fabricating methods. First, plural AAOs are produced at one time through simultaneous multi-surfaces anodization (SMSA), indicating mass-producibility of the AAOs with comparable qualities. Second, those AAOs can be separated from the aluminum (Al) substrate by applying stair-like reverse biases (SRBs) in the same electrolyte used for the SMSAs, implying simplicity and green technological characteristics. Finally, a unit sequence consisting of the SMSAs sequentially combined with SRBs-based detachment can be applied repeatedly to the same Al substrate, which reinforces the advantages of this strategy and also guarantees the efficient usage of natural resources.

## Video Link

The video component of this article can be found at <https://www.jove.com/video/56432/>

## Introduction

AAOs which were formed by anodizing Al substrate in an acidic electrolyte, have attracted great interest in diverse fundamental science and industry, for example, hard templates for nanotubes/nanowires<sup>1,2,3,4,5</sup>, energy storage devices<sup>6,7,8,9</sup>, bio-sensing<sup>10,11</sup>, filtering applications<sup>12,13,14</sup>, masks for evaporating and/or etching<sup>15,16,17</sup>, and capacitive humidity sensors<sup>18,19,20,21,22</sup>, owing to their self-ordered honeycomb structure, high aspect ratio of nanopores, and superior mechanical properties<sup>23</sup>. For applying the nanoporous AAOs to these various applications, they should be freestanding forms with a highly and long-range ordered array of nanopores. In this regard, strategies for obtaining AAOs must consider both formation (anodizing) and separation (detaching) procedures.

In the viewpoint of the AAO formation, mild anodization (hereafter referred as MA) was well established under sulfuric, oxalic, and phosphoric acid electrolytes<sup>23,24,25,26,27</sup>. However, MA processes exhibited low-yields of AAO fabrication due to their slow growth rate depending on relatively low intensities of anodic voltages, which would further deteriorate through a two-step MA process for improving nanopores' periodicity<sup>28,29</sup>. Thus, hard anodization (HA) techniques were proposed as alternatives of MA by applying higher anodic voltages (oxalic/sulfuric acid electrolyte) or using more concentrated electrolyte (phosphoric acid)<sup>30,31,32,33,34,35,36,37,38,39,40</sup>. HA processes show distinct enhancements of growth rates as well as periodic arrangements, whereas resulting AAOs became more fragile, and the density of nanopores were reduced<sup>30</sup>. In addition, an expensive cooling system is required for dissipating Joule's heating caused by high current density<sup>31</sup>. These results restrict the potential applicability of the AAOs via HA processes.

For separating an AAO from the corresponding surface of Al plate, selective chemical etching of the remaining Al substrate was most widely utilized in both the MA and HA processes using toxic chemicals, such as copper chloride<sup>35,39,41,42</sup> or mercury chloride<sup>16,17,43,44,45,46,47,48,49</sup>. However, this method induces disadvantageous side effects, *e.g.*, a longer reaction time proportional to the remaining thickness of the Al, contamination of AAO by heavy metal ions, harmful residues to human body/natural environments, and inefficient usage of valuable resources. Therefore, many attempts have been made for realizing direct detachment of an AAO. Although both cathodic voltage delamination<sup>50,51</sup> and anodic voltage pulse detachment<sup>7,41,42,52,53,54,55</sup> present a merit that the remaining Al substrate can be reused, the former technique takes almost comparable time with those in chemical etching methods<sup>50</sup>. Notwithstanding clear reduction of the processing time, harmful and highly reactive chemicals, for examples butanedione and/or perchloric acid, were used as detaching electrolytes in the latter techniques<sup>55</sup>, where an

additional cleaning procedure is needed because of the changing electrolyte between the anodizing and detaching procedure. Especially, the detaching behaviors and quality of the detached AAOs severely influence the thickness. In the case of the AAO with relatively thinner thickness, the detached one might contain cracks and/or apertures.

All the experimental approaches listed above have been applied to a "single-surface" of the Al specimen, excluding surface protecting/engineering purposes, and this feature of the conventional technologies exhibits critical limitations of the AAO fabrication in terms of yield as well as processibility, which also influences the potential applicability of the AAOs<sup>56,57</sup>.

To satisfy the increasing demands in the AAO-related fields in terms of facile, high yield, and green technological approaches, we previously reported on SMSA and direct detachment through SRBs under sulfuric<sup>56</sup> and oxalic<sup>57</sup> acid electrolyte, respectively. It is a well-known fact that plural AAOs can be formed on the multiple surfaces of the Al substrate immersed into acidic electrolytes. However, SRBs, a key distinction of our methods, enable the detachment of those AAOs from the corresponding multi-surfaces of the Al substrate in the same acidic electrolyte used for the SMSAs indicating mass-production, simplicity, and green technological characteristics. We would like to point out that SRBs-based detachment is an optimal strategy for plural AAOs fabricated by SMSAs<sup>56,57</sup> and even valid for relatively thinner thicknesses of AAOs<sup>57</sup> when compared with cathodic delamination (*i.e.*, constant reverse bias) on single-surface<sup>51</sup>. Finally, a unit sequence consisting of the SMSAs sequentially combined with SRBs-based detachment can be applied repeatedly to the same Al substrate, avoiding complicated procedures and toxic/reactive chemicals, which reinforces the advantages of our strategies and also guarantees the efficient usage of natural resources.

## Protocol

Please be aware of all the related materials safety data sheets (MSDS) before beginning. In spite of the eco-friendly nature of this protocol, a few acids and oxidizers are used in the corresponding procedures. Also, use all the proper personal protective equipment (lab coat, gloves, safety glasses, etc.).

### 1. Preparation of Solution

Note: After complete sealing of the solution-containing vessel, vigorous magnetic stirring was applied to all the solutions at room temperature in sufficient time.

#### 1. Preparation of perchloric acid solution

1. Mix 100 mL of perchloric acid ( $\text{HClO}_4$ , 60%) with 400 mL of absolute ethanol ( $\text{C}_2\text{H}_5\text{OH}$ , 100%) in 1 to 4 volume ratio.

#### 2. Preparation of chromic acid solution

1. Dissolve 9.0 g chromic oxide ( $\text{CrO}_3$ ) and 20.3 mL phosphoric acid ( $\text{H}_3\text{PO}_4$ , 85%) in 479.7 mL deionized (D.I.) water ( $\text{CrO}_3:\text{H}_3\text{PO}_4 = 0.18 \text{ M}:0.56 \text{ M}$ ).

#### 3. Preparation of sulfuric acid electrolyte

1. Mix 16.2 mL sulfuric acid ( $\text{H}_2\text{SO}_4$ , 98%) in 983.8 mL D.I. water resulting in molar concentration of 0.3 M.

#### 4. Preparation of oxalic acid electrolyte

1. Dissolve 27.012 g anhydrous oxalic acid ( $\text{C}_2\text{H}_2\text{O}_4$ ) in 1 L D.I. water resulting in molar concentration of 0.3 M.

### 2. Pretreatment of Al Substrate

#### 1. Machining Al specimen

1. Cut the purified Al specimen (>99.99% pure) into rectangular parallelepiped shape (width x height x thickness = 20.0 mm x 50.0 mm x 1.0 mm) with right angles between all the adjacent surfaces, which is referred as "substrate" hereafter.
2. Polish the multi-surfaces of the Al substrate mechanically using sandpaper with proper ISO/FEPA Grit Designation number more than P1000.

NOTE: See the **Supplementary Information** for more details.

#### 2. Simultaneous electropolishing on multi-surfaces of the Al substrate

1. Pour approximate 350 mL of perchloric acid ethanol solution into double jacket beaker with maximum capability of 600 mL. Then, immerse four-fifths of the Al substrate into perchloric acid solution.
2. Set the temperature of perchloric acid solution at  $7 \pm 0.1$  °C using a bath circulator connected to a double jacket beaker.
3. Clean the Al substrate through ultrasonication in acetone for 30-40 min, and rinse using acetone and D.I water a few times to remove organic residues on the surfaces of the Al substrate.
4. Dry the Al substrate using air-gun or nitrogen ( $\text{N}_2$ ) gas blow for eliminating residual solvents.  
NOTE: Natural drying under atmospheric environments is not be recommended because the solvent traces affect the electropolishing effects adversely.
5. Connect the Al substrate working electrode (W.E.) to the positive (+) port and the platinum (Pt) wire counter electrode (C.E.) to the negative (-) port of programmable DC power supply, using alligator clips. The Al substrate and Pt wire should be parallel to each other (See the **Figure S2**).
6. Apply forward bias of +20.0 V to the Al W.E. with respect to Pt C.E. for 2 - 4 min on average. Depending on the surface condition, such as contamination or roughness, the applying time could be maintained up to 5 min. Inspect all the surfaces immersed into the solution to check whether residues on the surface peel off and slide down into the solution. During this step, magnetic stirring is not recommended because inspection is difficult under stirring, and the solution flow might influence the electropolishing effect.  
NOTE: Do not electropolish for more than 5 min, which might deteriorate the surfaces.

Option: Recording current-time ( $I-t$ ) characteristics behavior via PC interface is helpful for monitoring the electropolishing procedure including abnormal points if they exist.

7. Stop applying bias and disconnect the alligator clips. Pick up the Al substrate and Pt electrode carefully from the electropolishing solution. Then, remove residual solution on the surface of the Al substrate using ethanol (95%) and D.I water a few times. If the electropolishing is performed properly, mirror-like finished surfaces of the Al substrate can be identified (See the **Figure S1** and **Figure S3**).
8. Store the electropolished Al substrate in ethanol (95%) until the next procedure to minimize surface oxidation.

### 3. Massive Fabrication of AAOs under Oxalic Acid Electrolyte

Note: For AAOs with a long-range arrangement of nanopores' periodicity, two-step SMSAs procedure were used, in which periodically textured Al multi-surfaces were obtaining through pre-SMSA, and then, main-SMSA was conducted for fabricating the highly qualified AAOs. Repetitive application of a unit sequence can keep producing plural and almost identical AAOs until the Al substrate remains. " $n$ " denotes number of the applied sequence.

#### 1. $n^{\text{th}}$ Pre-SMSA

1. Pour approximate 650 mL of oxalic acid aqueous solution with molar concentration of 0.3 M into a double jacket beaker with maximum capability of 1.0 L. Then, immerse about three quarters of the Al substrate into the oxalic acid solution.
2. Set the temperature of oxalic acid electrolyte at  $15 \pm 0.1$  °C using a bath circulator connected to a double jacket beaker.
3. Pick up the electropolished Al substrate from ethanol, and remove the residual solvent using an air-gun or  $N_2$  gas blow.
4. Connect the electropolished Al substrate to W.E. (+) and Pt wire to C.E. (-) of programmable DC power supply using an alligator clip. The Al substrate and Pt wire should be parallel to each other. Then, immerse the electropolished portion of the Al substrate into oxalic acid electrolyte.

NOTE: Make sure that enough space (e.g., approximate 1 cm) exists between the top of the acidic electrolyte and the bottom of the alligator clip connected to the Al substrate, otherwise severe corrosion occurs at the alligator clip connected position.

5. Apply anodic bias of +40.0 V to W.E. with respect to C.E. for more than 1-2 h under moderate magnetic stirring of 100-150 rpm for maintaining electrolyte temperature.

NOTE: If the Pre-SMSA time is too short, multi-surfaces of the Al substrate will not be textured properly.

Option: Recording  $I-t$  characteristics behavior via PC interface is helpful for understanding typical behaviors in SMSA.

6. Stop applying anodic bias after finishing pre-SMSA, and disconnect the alligator clips. Pick up the sample carefully from acidic electrolyte, and rinse the pre-SMSAed Al substrate using acetone and D.I water a few times.

#### 2. $n^{\text{th}}$ Pre-AAOs etching

1. Set the temperature of chromic acid aqueous solution at 60 - 65 °C.
2. Immerse the pre-SMSAed Al substrate into chromic acid solution for 1 - 2 h to remove pre-AAOs on the Al substrate.
3. Rinse the pre-AAOs removed Al substrate with acetone and D.I. water a few times. Measure the resistance of the Al substrate to confirm whether the pre-AAOs have been completely removed on the surface. If not, repeat the etching procedure again (step 3.2.2).

#### 3. $n^{\text{th}}$ Main-SMSA

1. Re-set up all the experimental conditions and connections as those used in step 3.1.  
NOTE: It should be noted that oxalic acid electrolyte can be used in a couple of sequences, and this does not influence the qualities of the main-AAOs. However, for quantitative comparisons, it is recommended that the electrolyte is used in one whole sequence, and then exchanged with a fresh one.
2. Apply anodic bias of +40.0 V to W.E. with respect to C.E.; applying time can be varied depending on a desirable thickness of AAO. AAO growth rate was estimated to be about 8.0 and 7.5  $\mu\text{m/h}$  on the front and back surface of the Al substrate at the electrolyte temperature of 15 °C, respectively (Refer to reference<sup>57</sup> for more details).

#### 4. $n^{\text{th}}$ SRBs-detachment

1. Stop applying the anodic bias and stirring after finishing the main-SMSA, and connect the main-SMSAed Al substrate to C.E. (-) and Pt wire to W.E. (+) of the programmable DC power supply by switching each alligator clip.
2. Apply the SRBs, and inspect typical bubbling effects along to the multi-edges of the Al substrate covered with main-AAOs. Details of SRBs condition, such as intensity of the beginning RB, number of stairs, and duration in each stair, are closely correlated with the thickness of main-AAOs. For main-AAOs thicker than 60  $\mu\text{m}$ , stair in SRBs was controlled from -21 V to -24 V with the increment of -1 V and without time interval between adjacent stairs. The duration for -21 V, -22 V, and -23 V was fixed at 10 min, and the final stair of -24 V was maintained until the detaching procedure completed (See reference<sup>57</sup> for more details including the case of thinner AAOs).  
NOTE: It is highly recommended for a beginner to utilize PC interfaced control of SRBs and record the  $I-t$  characteristic curves during this procedure.
3. Quit applying SRBs after finishing the detachment, and disconnect the alligator clips. Pick up the sample carefully from acidic electrolyte, and rinse them carefully with acetone and D.I water a sufficient number of times.
4. Separate each AAO from corresponding Al surface completely. Right after step 3.4.3, upper parts of the detached AAOs are still connected to the Al substrate, which should be manually broken.

#### 5. $n^{\text{th}}$ Residual alumina etching

1. Set the temperature of chromic acid solution at 60-65 °C, and immerse the AAOs-detached Al substrate for about 30 min to eliminate residual alumina.
2. Pick up the etched Al substrate, and rinse with acetone and D.I. water a few times. Measure the resistance to confirm complete removal of residual alumina. If not, repeat step 3.5.2.

#### 6. $n+1^{\text{th}}$ sequence

1. Go to step 3.1, and repeat the whole sequence using the residual alumina-etched Al substrate.

## 4. Massive Fabrication of AAOs under Sulfuric Acid Electrolyte

NOTE: In this section, clearly different conditions from those in step 3 are pointed out.

### 1. $n^{\text{th}}$ Pre-SMSA

1. Pour approximate 650 mL of sulfuric acid aqueous solution (0.3 M) into a double jacket beaker with maximum capability of 1.0 L. Then, about three quarters of the Al substrate is immersed into the sulfuric acid solution.
2. Set the temperature of the electrolyte at  $0 \pm 0.1$  °C.
3. Remove the residual solvent on the electropolished Al substrate using an air-gun or  $\text{N}_2$  gas blow, and connect the Al substrate to a programmable DC power supply using alligator clips (Refer to step 3.1.4)
4. Apply anodic bias of +25.0 V to W.E. with respect to C.E. for more than 1 - 2 h under moderate magnetic stirring (100 - 150 rpm).
5. Quit applying the anodic bias after finishing pre-SMSA, and disconnect the alligator clips. Pick up and rinse the pre-SMSAed Al substrate using acetone and D.I water a few times.  
NOTE: For  $n^{\text{th}}$  Pre-AAOs etching, refer to step 3.2.

### 2. $n^{\text{th}}$ Main-SMSA

1. Re-set up all the experimental conditions and connections as those used in step 4.1.
2. Apply the same anodic bias. Applying time can be varied depending on a desirable AAO thickness. AAO growth rate was estimated to be about 5.3  $\mu\text{m}/\text{h}$  (Refer to reference<sup>56</sup> for more details).

### 3. $n^{\text{th}}$ SRBs-detachment

1. Quit applying the anodic bias and stirring after finishing the main-SMSA, and connect the main-SMSAed Al substrate to C.E. (-) and Pt wire to W.E. (+) of programmable DC power supply by switching each alligator clip.
2. Apply SRBs, and inspect typical bubbling effects along to the multi-edges of the sample. Stair in SRBs was controlled from -15 V to -17 V with the increment of -1 V and without time interval between adjacent stairs. The duration for -15 V and -16 V was fixed at 10 min, and final stair of -17 V was maintained until the detaching procedure completed.  
NOTE: Based on the more fragile nature of AAOs fabricated under sulfuric acid electrolyte, the current level was abruptly increased at the detaching moments accompanied with noticeable clicking sounds.
3. Quit applying the SRBs after finishing the detachment, and disconnect the alligator clips. Pick up the sample carefully from the acidic electrolyte, and rinse carefully with acetone and D.I water a sufficient number of times.
4. Separate each AAO from the corresponding Al surface mechanically by breaking the upper parts of as-detached AAOs.  
NOTE: For  $n^{\text{th}}$  Residual alumina etching refer to step 3.5.

### 4. $n+1^{\text{th}}$ sequence

1. Go to step 4.1, and repeat the whole sequence using the residual alumina-etched Al substrate.

## Representative Results

Flow chart of  $n^{\text{th}}$  AAO fabricating sequence mainly consisting of two-step SMSAs, SRBs-detachment, and related chemical etching was presented schematically in **Figure 1a**. Each inset show a scanning electron microscope (SEM) image of the corresponding surface morphology at each individual procedure and a photograph taken immediately after SRBs-detachment. A schematic illustration after the total 5<sup>th</sup> repetition of the unit sequence exhibited advantages of SMSA and SRBs-based strategies (**Figure 1b**). *I-t* characteristic curves of the pre- and main-SMSAs up to the 5<sup>th</sup> sequences were compared in **Figure 2a** and **Figure 2b**, respectively. A comparison of *I-t* characteristic curves from each SRBs-detaching procedure are shown in **Figure 2c**. Photograph and corresponding SEM images of the main-AAOs obtained from front and back surfaces under oxalic and sulfuric acid electrolytes are presented in **Figure 3** and **Figure 4**, respectively.

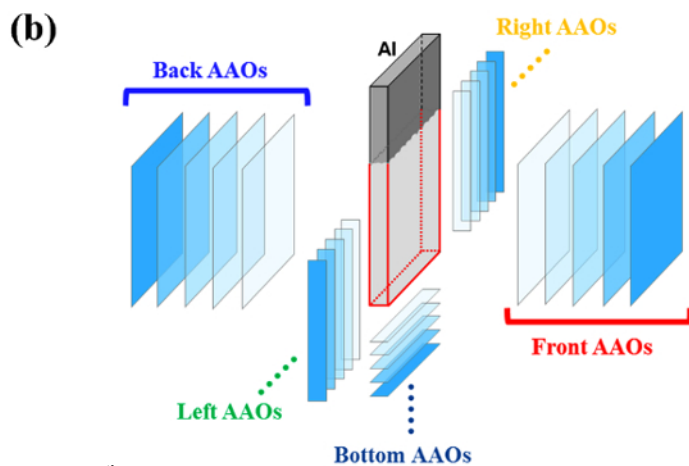
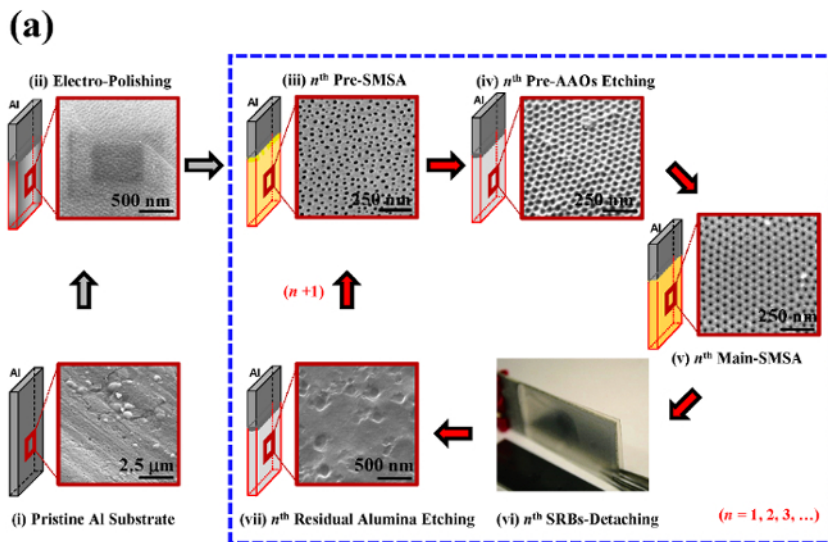


**Figure 1:**  $n^{\text{th}}$  AAOs fabrication procedures ( $n = 1, 2, 3 \dots$ ). (a) Schematic flow chart including corresponding SEM images in  $n^{\text{th}}$  AAOs fabricating sequence: (i) Pristine Al substrate, (ii) Electro polishing, (iii)  $n^{\text{th}}$  pre-SMSA, (iv)  $n^{\text{th}}$  pre-AAOs etching, (v)  $n^{\text{th}}$  main-SMSA, (vi)  $n^{\text{th}}$  SRBs-detaching, (vii)  $n^{\text{th}}$  residual alumina etching. A unit sequence was depicted using blue-dashed box. (b) Schematic illustration showing that plural AAOs with equal dimensions of corresponding surfaces were successfully obtained from multi-surfaces of a single Al plate through 5<sup>th</sup> repetitive applications of the unit sequence. [Please click here to view a larger version of this figure.](#)

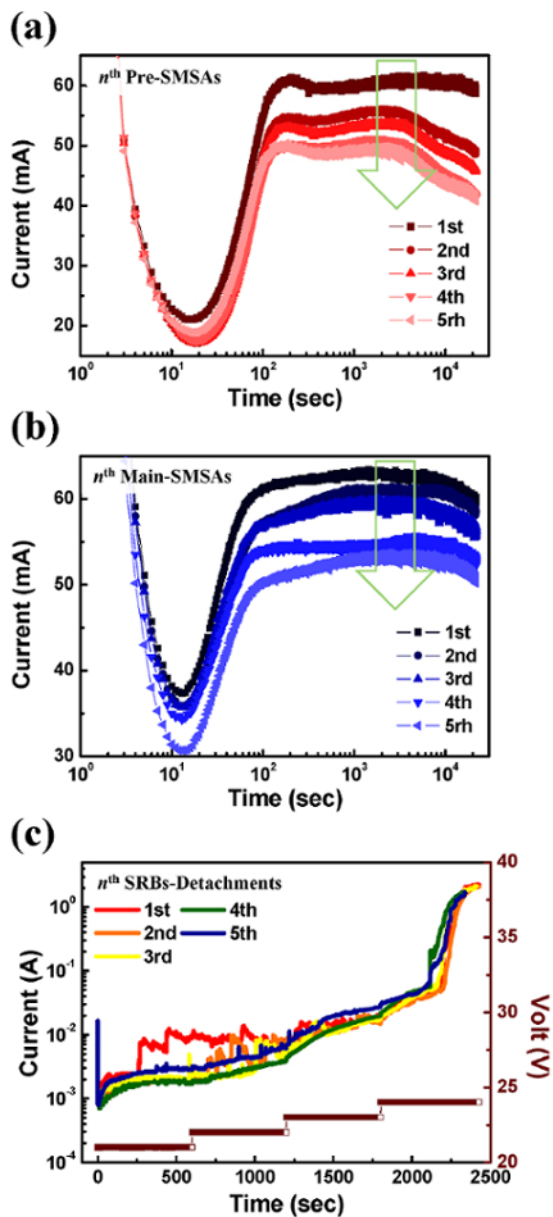
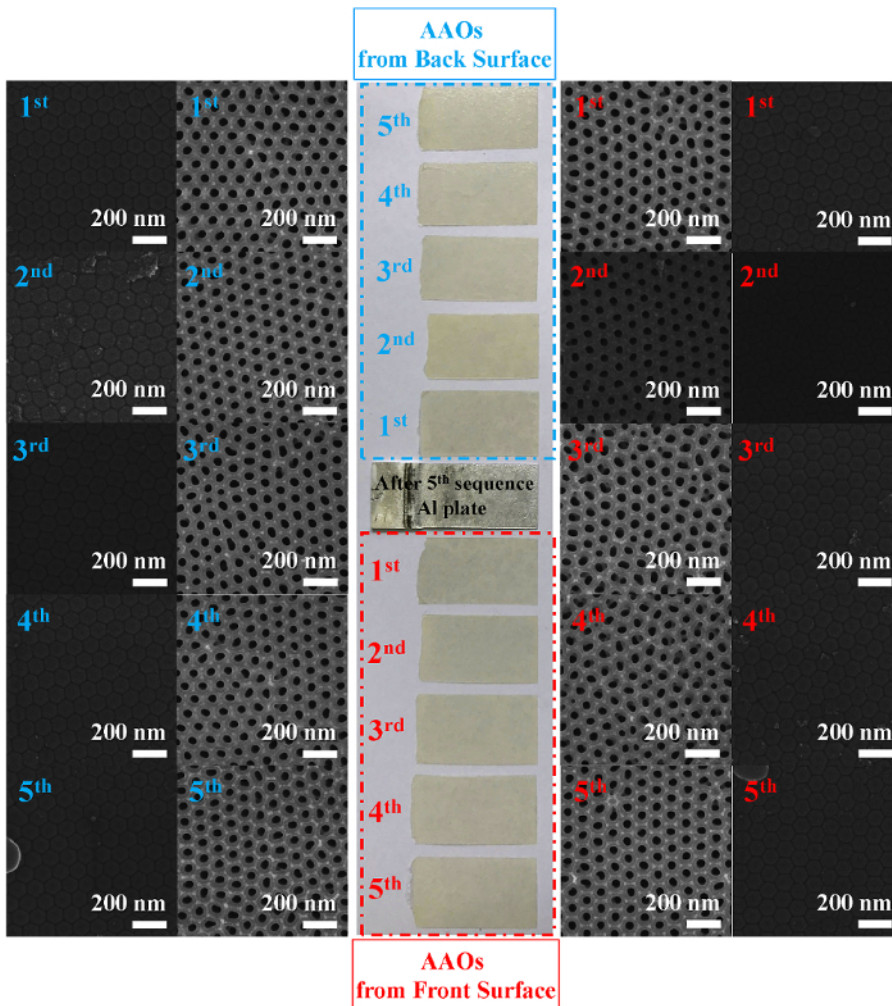
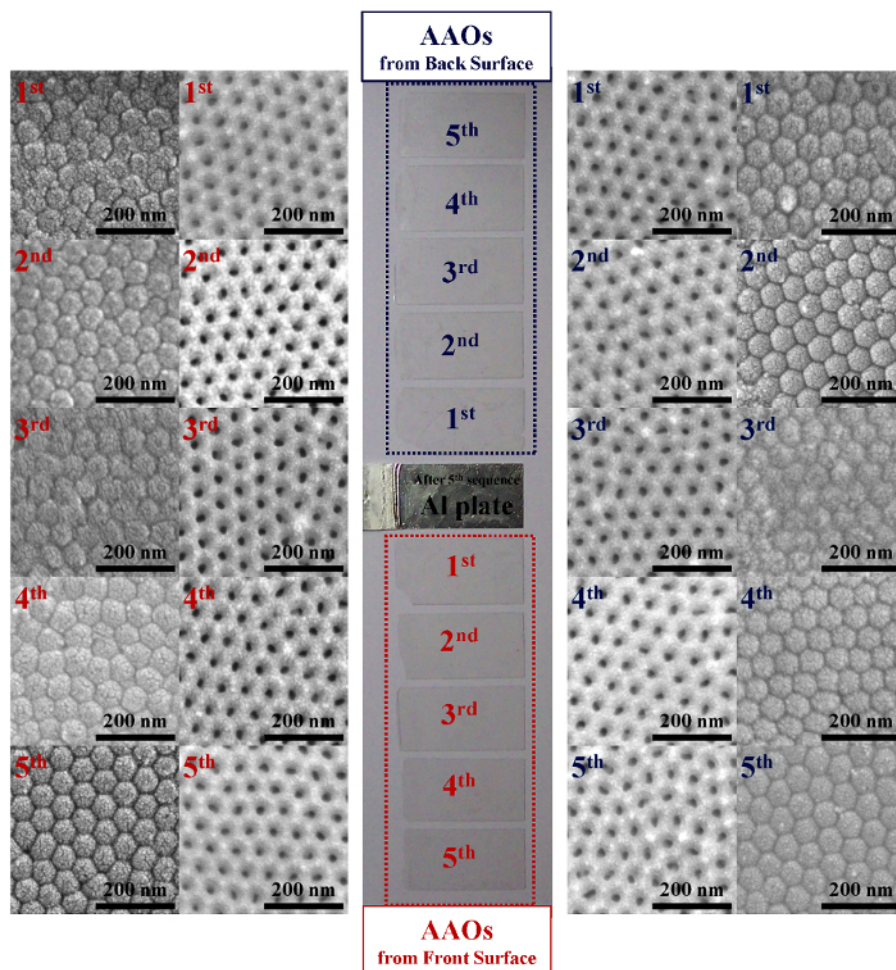


Figure 2: Peculiar behaviors during two-step SMSAs and SRBs-detachments of AAOs under oxalic acid electrolyte at 15 °C. *I-t* characteristic curves of (a) pre- and (b) main-SMSAs from 1<sup>st</sup> to 5<sup>th</sup> sequences, respectively. (c) *I-t* characteristic curves of SRBs-detaching procedures from 1<sup>st</sup> to 5<sup>th</sup> sequences. [Please click here to view a larger version of this figure.](#)



**Figure 3: Photograph of the remaining Al substrate and main-AAOs after 5<sup>th</sup> repetitive applications of the unit sequence under oxalic acid electrolyte.** AAOs obtained from front and back surfaces were distinguished by red- and blue-dashed boxes, respectively. Insets: Open-pore and barrier side SEM images of the corresponding 1<sup>st</sup> to 5<sup>th</sup> main-AAOs. [Please click here to view a larger version of this figure.](#)



**Figure 4:** Photograph of the remaining Al substrate and main-AAOs after 5<sup>th</sup> repetitive applications of the unit sequence under sulfuric acid electrolyte. AAOs obtained from front and back surfaces were distinguished by red- and blue-dashed boxes, respectively. Insets: Open-pore and barrier side SEM images of the corresponding 1<sup>st</sup> to 5<sup>th</sup> main-AAOs. [Please click here to view a larger version of this figure.](#)

**Supplementary Information:** [Please click here to download this file.](#)

## Discussion

In this paper, we successfully demonstrated a facile, high yield, and environmentally clean method to fabricate nanoporous AAOs through SMSA and SRBs-detachment, which could be repeated to the same Al substrate for significantly enhancing mass-productibility as well as usability of limited natural resource. As shown in the flow chart of **Figure 1a**, our AAO fabricating strategy is based on the conventional two-step anodization, which was modified on multi-surfaces situation. Individual procedures functioned well independent of the other surfaces, because electric fields in the electropolishing and two-step SMSAs procedures were formed in the normal directions on the multi-surfaces, where the electrochemical reaction occurs simultaneously. In this point of view, position of each surface and corresponding AAO will be defined with respect to the counter electrode, as shown in **Figure 1b**; e.g., "Front" designate a surface confronting the Pt counter electrode, and so on.

Pristine Al substrate showed rougher surfaces due to mechanical polishing, which became much smoother after electropolishing procedure. Each surface of the electropolished Al substrate looked like a mirror in macroscale, however, it was covered with irregularly distributed nanoscale concaves as shown in the inset (ii) of **Figure 1a**. Therefore, not only every cleaning but also drying treatment were also very important, owing to the fact that solvent traces could significantly affect surface morphologies in procedures after electropolishing. Once deteriorated, surfaces never recovered, and kept the poor morphologies. In this regard, excessive electropolishing treatment would not be good either. If electropolishing time is too long, periodically arranged wavy valleys were formed on the entire Al surfaces, which could increase an adhesive strength between AAOs and Al. A unit sequence depicted by a blue-dashed box shown in **Figure 1a** consists of  $n^{\text{th}}$  pre-SMSA,  $n^{\text{th}}$  pre-AAOs etching,  $n^{\text{th}}$  main-SMSA,  $n^{\text{th}}$  SRBs-detachment, and  $n^{\text{th}}$  residual alumina etching, where  $n$  is number of the applied sequence ( $n = 1, 2, 3, \dots$ ).

**Figure 2** compares the  $I-t$  characteristic curves of pre-/main-SMSA and SRBs-detachment from 1<sup>st</sup> to 5<sup>th</sup> sequences. In both SMSAs, the current level gradually decreased with increasing applying time. These typical features were only observed in a multi-surfaces situation attributing to the gradual reduction of total anodizing area as well as accumulation of mechanical stresses due to the viscous flow<sup>23,58</sup> and volume expansion<sup>23,59,60,61,62</sup> during simultaneous formations of plural AAOs<sup>56,57</sup>. Previous reports on these SMSA and SRBs-detachment proposed



the stress-released direct detaching mechanism, which could be further optimized through appropriate SRBs conditions for relatively thinner thickness of AAO (Refer to reference<sup>57</sup> for more details).

An intuitive schematic illustration implying massive producibility is successfully realized in **Figure 3** and **Figure 4** exhibiting results of about total 5<sup>th</sup> times iterations of the unit sequence under oxalic and sulfuric acid electrolyte, respectively. Each photograph clearly shows that all the AAOs having the exact equal dimensions to those of corresponding front and back surfaces (See the **Supplementary Information** for the AAOs detached from sides and bottom surfaces). Barrier side SEM images of all sequences indicate that cleavage planes are beneath the barrier oxides in both acidic electrolytes, which are similar results about cathodic delamination of a relatively thicker AAO on mono-surface<sup>50,51</sup>. As an alternative approach for obtaining AAO with through-hole structures (*i.e.*, without barrier oxide), anodic voltage pulse detachment using another detaching electrolyte<sup>7,41,42,52,53,54,55</sup> or two-layer anodization incorporating normal AAO into a sacrificial one fabricated from acidic electrolyte of extremely high concentration (12.0 M)<sup>63</sup> might be taken into consideration.

The SMSA and SRBs-based strategy appears to possess an acid-type independent nature, therefore, its various advantages and strengths are worth expanding into phosphoric acid electrolyte and/or HA condition, which will enrich the potentials of nanoporous AAOs toward more versatile applications.

## Disclosures

This research was supported in part by the National Research Foundation of Korea (NRF) grant funded by the Korea government (MSIP) (No. 2016R1C1B1016344 and 2016R1E1A2915664).

## Acknowledgements

The authors have nothing to disclose.

## References

1. Hong, Y. K. *et al.* Tuning and enhancing photoluminescence of light-emitting polymer nanotubes through electron-beam irradiation. *Adv. Funct. Mater.* **19** (4), 567-572 (2009).
2. Hong, Y. K. *et al.* Fine Characteristics Tailoring of Organic and Inorganic Nanowires Using Focused Electron-Beam Irradiation. *Angew. Chem. Int. Ed.* **50** (16), 3734-3738 (2011).
3. Lee, J. H. *et al.* Iron-gold barcode nanowires. *Angew. Chem. Int. Ed.* **46** (20), 3663-3667 (2007).
4. Qin, L., Banholzer, M. J., Millstone, J. E. Mirkin, C. A. Nanodisk codes. *Nano Lett.* **7** (12), 3849-3853 (2007).
5. Park, D. H., Kim, M. S. Joo, J. Hybrid nanostructures using  $\pi$ -conjugated polymers and nanoscale metals: synthesis, characteristics, and optoelectronic applications. *Chem. Soc. Rev.* **39** (7), 2439-2452 (2010).
6. Ahn, Y. K. *et al.* Enhanced electrochemical capabilities of lithium ion batteries by structurally ideal AAO separator. *J. Mater. Chem. A.* **3** (20), 10715-10719 (2015).
7. Chen, J., Wang, S., Ding, L., Jiang, Y. Wang, H. Performance of through-hole anodic aluminum oxide membrane as a separator for lithium-ion battery. *J. Membr. Sci.* **461** 22-27 (2014).
8. Gao, Y. *et al.* Three-dimensional nanotube electrode arrays for hierarchical tubular structured high-performance pseudocapacitors. *Nanoscale.* **8** (27), 13280-13287 (2016).
9. Hu, J. *et al.* Dual-template ordered mesoporous carbon/Fe<sub>2</sub>O<sub>3</sub> nanowires as lithium-ion battery anodes. *Nanoscale.* **8** (26), 12958-12969 (2016).
10. Kim, K. *et al.* Externally controlled drug release using a gold nanorod contained composite membrane. *Nanoscale.* **8** (23), 11949-11955 (2016).
11. Poplausks, R. *et al.* Electrochemically etched sharp aluminium probes with nanoporous aluminium oxide coatings: Demonstration of addressed DNA delivery. *RSC Adv.* **4** (89), 48480-48485 (2014).
12. Chen, X., Qiu, M., Ding, H., Fu, K. Fan, Y. A reduced graphene oxide nanofiltration membrane intercalated by well-dispersed carbon nanotubes for drinking water purification. *Nanoscale.* **8** (10), 5696-5705 (2016).
13. Dervin, S., Dionysiou, D. D. Pillai, S. C. 2D nanostructures for water purification: graphene and beyond. *Nanoscale.* **8** (33), 15115-15131 (2016).
14. Han, K., Heng, L., Wen, L. Jiang, L. Biomimetic heterogeneous multiple ion channels: a honeycomb structure composite film generated by breath figures. *Nanoscale.* **8** (24), 12318-12323 (2016).
15. Kim, J., Kim, Y. H., Choi, S. H. Lee, W. Curved Silicon Nanowires with Ribbon-like Cross Sections by Metal-Assisted Chemical Etching. *ACS Nano.* **5** (6), 5242-5248 (2011).
16. Zeng, Z. *et al.* Fabrication of Graphene Nanomesh by Using an Anodic Aluminum Oxide Membrane as a Template. *Adv. Mater.* **24** (30), 4138-4142 (2012).
17. Lim, N. *et al.* A tunable sub-100 nm silicon nanopore array with an AAO membrane mask: reducing unwanted surface etching by introducing a PMMA interlayer. *Nanoscale.* **7** (32), 13489-13494 (2015).
18. Zhang, J., Liu, X., Neri, G. Pinna, N. Nanostructured Materials for Room-Temperature Gas Sensors. *Adv. Mater.* **28** (5), 795-831 (2016).
19. Blank, T. A., Eksperiandova, L. P. Belikov, K. N. Recent trends of ceramic humidity sensors development: A review. *Sens. Actuators B.* **228** 416-442 (2016).
20. Kim, Y. *et al.* Capacitive humidity sensor design based on anodic aluminum oxide. *Sens. Actuators B.* **141** (2), 441-446 (2009).
21. Mahboob, M. R., Zargar, Z. H. Islam, T. A sensitive and highly linear capacitive thin film sensor for trace moisture measurement in gases. *Sens. Actuators B.* **228** 658-664 (2016).
22. Sharma, K. Islam, S. S. Optimization of porous anodic alumina nanostructure for ultra high sensitive humidity sensor. *Sens. Actuators B.* **237** 443-451 (2016).

23. Lee, W. Park, S.-J. Porous Anodic Aluminum Oxide: Anodization and Templated Synthesis of Functional Nanostructures. *Chem. Rev.* **114** (15), 7487-7556 (2014).
24. Keller, F., Hunter, M. Robinson, D. Structural features of oxide coatings on aluminum. *J. Electrochem. Soc.* **100** (9), 411-419 (1953).
25. Diggle, J. W., Downie, T. C. Goulding, C. W. Anodic oxide films on aluminum. *Chem. Rev.* **69** (3), 365-405 (1969).
26. Sullivan, J. P. Wood, G. C. The Morphology and Mechanism of Formation of Porous Anodic Films on Aluminium. *Proc. R. Soc. London A.* **317** (1531), 511-543 (1970).
27. Thompson, G. E. Wood, G. C. Porous anodic film formation on aluminium. *Nature.* **290** (5803), 230-232 (1981).
28. Masuda, H. Fukuda, K. Ordered Metal Nanohole Arrays Made by a Two-Step Replication of Honeycomb Structures of Anodic Alumina. *Science.* **268** (5216), 1466-1468 (1995).
29. Masuda, H. Satoh, M. Fabrication of Gold Nanodot Array Using Anodic Porous Alumina as an Evaporation Mask. *Jpn. J. Appl. Phys.* **35** (1 B), L126-L129 (1996).
30. Chu, S. Z., Wada, K., Inoue, S., Isogai, M. Yasumori, A. Fabrication of Ideally Ordered Nanoporous Alumina Films and Integrated Alumina Nanotubule Arrays by High-Field Anodization. *Adv. Mater.* **17** (17), 2115-2119 (2005).
31. Lee, W., Ji, R., Gösele, U. Nielsch, K. Fast fabrication of long-range ordered porous alumina membranes by hard anodization. *Nature Mater.* **5** (9), 741-747 (2006).
32. Li, Y., Zheng, M., Ma, L. Shen, W. Fabrication of highly ordered nanoporous alumina films by stable high-field anodization. *Nanotechnology.* **17** (20), 5101-5105 (2006).
33. Li, Y. B., Zheng, M. J. Ma, L. High-speed growth and photoluminescence of porous anodic alumina films with controllable interpore distances over a large range. *Appl. Phys. Lett.* **91** (7), 073109 (2007).
34. Lee, W. *et al.* Structural engineering of nanoporous anodic aluminium oxide by pulse anodization of aluminium. *Nature Nanotech.* **3** (4), 234-239 (2008).
35. Li, Y., Ling, Z. Y., Chen, S. S. Wang, J. C. Fabrication of novel porous anodic alumina membranes by two-step hard anodization. *Nanotechnology.* **19** (22), 225604 (2008).
36. Schwirn, K. *et al.* Self-Ordered Anodic Aluminum Oxide Formed by H<sub>2</sub>SO<sub>4</sub> Hard Anodization. *ACS Nano.* **2** (2), 302-310 (2008).
37. Yao, Z., Zheng, M., Ma, L. Shen, W. The fabrication of ordered nanoporous metal films based on high field anodic alumina and their selected transmission enhancement. *Nanotechnology.* **19** (46), 465705 (2008).
38. Lee, W., Kim, J. C. Cösele, U. Spontaneous Current Oscillations during Hard Anodization of Aluminum under Potentiostatic Conditions. *Adv. Funct. Mater.* **20** (1), 21-27 (2010).
39. Yi, L., Zhiyuan, L., Shuoshuo, C., Xing, H. Xinhua, H. Novel AAO films and hollow nanostructures fabricated by ultra-high voltage hard anodization. *Chem. Commun.* **46** (2), 309-311 (2010).
40. Kim, M., Ha, Y. C., Nguyen, T. N., Choi, H. Y. Kim, D. Extended self-ordering regime in hard anodization and its application to make asymmetric AAO membranes for large pitch-distance nanostructures. *Nanotechnology.* **24** (50), 505304 (2013).
41. Chen, W., Wu, J. S., Yuan, J. H., Xia, X. H. Lin, X. H. An environment-friendly electrochemical detachment method for porous anodic alumina. *J. Electroanal. Chem.* **600** (2), 257-264 (2007).
42. Gao, L., Wang, P., Wu, X., Yang, S. Song, X. A new method detaching porous anodic alumina films from aluminum substrates. *J. Electroceram.* **21** (1-4 SPEC. ISS.), 791-794 (2008).
43. Asoh, H., Nishio, K., Nakao, M., Tamamura, T. Masuda, H. Conditions for Fabrication of Ideally Ordered Anodic Porous Alumina Using Pretextured Al. *J. Electrochem. Soc.* **148** (4), B152-B156 (2001).
44. Wu, M. T., Leu, I. C. Hon, M. H. Effect of polishing pretreatment on the fabrication of ordered nanopore arrays on aluminum foils by anodization. *J. Vac. Sci. Technol., B.* **20** (3), 776-782 (2002).
45. Asoh, H., Ono, S., Hirose, T., Nakao, M. Masuda, H. Growth of anodic porous alumina with square cells. *Electrochim. Acta.* **48** (20-22), 3171-3174 (2003).
46. Masuda, H. *et al.* Ordered Mosaic Nanocomposites in Anodic Porous Alumina. *Adv. Mater.* **15** (2), 161-164 (2003).
47. Chu, S. Z. *et al.* Large-Scale Fabrication of Ordered Nanoporous Alumina Films with Arbitrary Pore Intervals by Critical-Potential Anodization. *J. Electrochem. Soc.* **153** (9), B384-B391 (2006).
48. Byun, J., Lee, J. I., Kwon, S., Jeon, G. Kim, J. K. Highly Ordered Nanoporous Alumina on Conducting Substrates with Adhesion Enhanced by Surface Modification: Universal Templates for Ultrahigh-Density Arrays of Nanorods. *Adv. Mater.* **22** (18), 2028-2032 (2010).
49. Gong, J., Butler, W. H. Zangari, G. Tailoring morphology in free-standing anodic aluminium oxide: Control of barrier layer opening down to the sub-10 nm diameter. *Nanoscale.* **2** (5), 778-785 (2010).
50. Schneider, J. J., Engstler, J., Budna, K. P., Teichert, C. Franzka, S. Freestanding, highly flexible, large area, nanoporous alumina membranes with complete through-hole pore morphology. *Eur. J. Inorg. Chem.* **2005** (12), 2352-2359 (2005).
51. Choudhary, E. Szalai, V. Two-step cycle for producing multiple anodic aluminum oxide (AAO) films with increasing long-range order. *RSC Adv.* **6** (72), 67992-67996 (2016).
52. Yuan, J. H., He, F. Y., Sun, D. C. Xia, X. H. A Simple Method for Preparation of Through-Hole Porous Anodic Alumina Membrane. *Chem. Mater.* **16** (10), 1841-1844 (2004).
53. Yuan, J. H., Chen, W., Hui, R. J., Hu, Y. L. Xia, X. H. Mechanism of one-step voltage pulse detachment of porous anodic alumina membranes. *Electrochim. Acta.* **51** (22), 4589-4595 (2006).
54. Zhao, S., Chan, K., Yelon, A. Veres, T. Preparation of open-through anodized aluminium oxide films with a clean method. *Nanotechnology.* **18** (24), 245304 (2007).
55. Brudzisz, A., Brzózka, A. Sulka, G. D. Effect of processing parameters on pore opening and mechanism of voltage pulse detachment of nanoporous anodic alumina. *Electrochim. Acta.* **178** 374-384 (2015).
56. Hong, Y. K., Kim, B. H., Kim, D. I., Park, D. H. Joo, J. High-yield and environment-minded fabrication of nanoporous anodic aluminum oxide templates. *RSC Adv.* **5** (34), 26872-26877 (2015).
57. Jeong, S. H. *et al.* Massive, eco-friendly, and facile fabrication of multi-functional anodic aluminum oxides: application to nanoporous templates and sensing platforms. *RSC Adv.* **7** (8), 4518-4530 (2017).
58. Houser, J. E. Hebert, K. R. The role of viscous flow of oxide in the growth of self-ordered porous anodic alumina films. *Nature Mater.* **8** (5), 415-420 (2009).
59. Jessensky, O., Müller, F. Gösele, U. Self-organized formation of hexagonal pore arrays in anodic alumina. *Appl. Phys. Lett.* **72** (10), 1173-1175 (1998).

60. Li, F., Zhang, L., Metzger, R. M. On the Growth of Highly Ordered Pores in Anodized Aluminum Oxide. *Chem. Mater.* **10** (9), 2470-2480 (1998).
61. Li, A. P., Müller, F., Bimer, A., Nielsch, K., Gösele, U. Hexagonal pore arrays with a 50-420 nm interpore distance formed by self-organization in anodic alumina. *J. Appl. Phys.* **84** (11), 6023-6026 (1998).
62. Nielsch, K., Choi, J., Schwirn, K., Wehrspohn, R. B., Gösele, U. Self-ordering Regimes of Porous Alumina: The 10% Porosity Rule. *Nano Lett.* **2** (7), 677-680 (2002).
63. Yanagishita, T., Masuda, H. High-Throughput Fabrication Process for Highly Ordered Through-Hole Porous Alumina Membranes Using Two-Layer Anodization. *Electrochim. Acta.* **184** 80-85 (2015).